Article

Integrated Photovoltaics Potential for Passenger Cars: A Focus on the Sensitivity to Electrical Architecture Losses

Fathia Karoui *, Bertrand Chambion, Fabrice Claudon and Benjamin Commault

Univ. Grenoble Alpes, CEA, LITEN, INES, 73375 Le Bourget du Lac, France
* Correspondence: fathia.karoui@cea.fr

Abstract: Vehicle integrated photovoltaics (VIPV) are among the identified solutions to reduce the environmental impacts of the transport sector. The model developed here simulates the VIPV system. It considers various usage patterns and vehicle types, several characteristics of the photovoltaic system and all the losses that may decrease energy yield. Focusing on a passenger car, simulations indicate the order of influence of the parameters on the outputs of the model: geographic locality, shading, thresholds due to extra-consumption needed to charge the vehicle's battery from the photovoltaic (PV) system and occurrence of recharge with the grid. With technology projections for 2030, with 30% shading, VIPV will cover a distance of up to 1444 km per year. This represents up to 12% of the driven mileage. For the best month, it can reach up to 14 km/day. For average Europe and realistic conditions, VIPV cover 648 km per year. Life cycle assessment (LCA) of a solarized passenger car shows a negative balance for a low-carbon electricity mix and average solar irradiance. In favorable conditions, the carbon footprint is up to 489 kg of CO_2-equivalent avoided emissions on a 13-year lifespan. Beyond the focus on km and LCA, VIPV may provide useful functions in non-interconnected zones and for resilience in disaster areas.

Keywords: VIPV; passenger car; life cycle assessment; mileage; electrical architecture; model; shading; carbon footprint

1. Introduction

Recently, the market share of electric vehicles (EVs) has increased. Meanwhile, the European Commission decided to end the sale of new diesel and petrol cars and vans by 2035 [1]. This decision will accelerate the production and sale of EVs. Therefore, research has been conducted on different methods allowing the optimization of the use of such vehicles. Mawonou et al. (2021) [2] developed an algorithm for the estimation of the state of health of EV batteries. They randomly selected 186 cars from a big database of more than 180,000 vehicles for learning of a random forest algorithm. Shen et al. (2022) [3] worked on the use pattern of EVs and load forecasting. Jirdehi et Tabar (2023) [4] optimized EV infrastructures integrated with renewable energies and implemented a demand-side strategy considering uncertainties.

Vehicle integrated photovoltaics (VIPV) are one of the investigated solutions to reduce the environmental impact of the transport sector. Many projects on VIPV have been carried out recently. Commault et al. (2021) [5] showed that the number of VIPV projects is increasing, especially car-based ones. They discussed the benefits and weaknesses of several photovoltaic (PV) cell and module technologies and gave recommendations for large-scale applications of such technologies.

Karoui et al. (2023) [6], recently published a study on the performance evaluation of electric bus solar roof integration. This study provides the simulation results for two localities: Malaga (best-case Europe) and Paris (average Europe) with different shading losses and two architectures for using PVs. It was shown that adding VIPV on a city bus allows covering between 3711 km and 9739 km per year. The life cycle assessment of the

studied solutions shows neutral to high gains. The avoided gas emissions are up to 28 T of CO_2-equivalent on a 20-year lifetime.

Other studies include the impact of shading on the performance of VIPV. Thiel et al. (2022) [7] estimated the energy performance of solar integration on a personal vehicle and on a distribution van in various climatic conditions without shading. They showed that photovoltaics can provide up to 35% of the driven distance. Sagaria et al. [8] study the solar energy interactions between five categories of vehicles and use configurations of VIPV. They consider shading but only in the sunny city of Lisbon in Portugal. Lodi et al. (2018) [9] from the European Commission's Joint Research Centre showed a PV use factor of 58% for passenger cars. This study allowed the European Commission to fix the value of shading losses for eco-innovation at 49% [10] to extrapolate the results to other locations in Europe. Arun et al. (2019) [11] studied the influence of partial shading in VIPV systems and the variation in output power with different forms of shading for a car. They simulated the maximum power point tracker (MPPT) with and without a boost converter. Brito et al. (2021) [12] have contributed to shading studies by giving an average of 52% irradiance loss during parking and an average of 26% during driving cycles in an urban environment in Lisbon. They calculated the average daily distance covered by VIPV in a year to be between 10 and 18 km/day/kWp.

For a passenger car, there are some losses due to the curvature of the solar panel. Ota et al. [13,14] proposed a methodology to characterize commercial solar roof top shapes, with a direct link to the potential PV coverage ratio. For a radius of curvature of 1 m, the coverage ratio is 96%. In this configuration, the applicable curve correction factor is 0.92 for generated energy as compared to a flat module.

The useful energy from VIPV depends also on the occurrence of recharge using the grid. Birnie et al. [15] studied the influence of plugging the electric vehicle to the grid at the work place during daylight hours. They showed a 75% loss of the available PV energy from VIPV. Thus, the vehicle's battery is recharged with the grid at night in this study. In the calculations, the frequency of recharge with the grid is a variable parameter.

Finally, the energy loss in the electronic components which allow charging the main battery of the vehicle using PV has an influence on VIPV performance. The authors have already partially shown this influence for a city bus [6], demonstrating that in this case directly charging the PV in the main battery is better than charging the low voltage battery first and periodically transfer energy from a low-voltage to high-voltage battery. This paper will study this question more deeply in Section 3.2 for a passenger car.

In this paper, we propose to consider all the factors that may influence the performance of VIPV on a passenger car. These factors are location, shading share, charge architecture, power thresholds for using PV, curvature of the solar panel and frequency of recharge with the grid. This study provides the performance of VIPV in terms of the PV energy supplied to the engine, the distance covered by the VIPV and CO_2 emissions estimated using life cycle assessment (LCA).

This paper contributes to the state of the art by evaluating the performance of VIPV on a passenger car in European countries. It considers the following factors:

- The daily use patterns which may vary during the week and the year;
- The monthly variations in solar irradiance and their hourly distribution;
- The PV panel's curvature;
- The solar panel's ageing;
- The shading;
- The system's effectiveness;
- Three architectures to transfer energy from the PV to the battery;
- Battery fullness due to the frequency of recharge with the grid and to rest days.

The energy/distance simulation model gives inputs to the life cycle analysis process, which allows the calculation of avoided carbon emissions.

This article is structured in five sections. Section 2 describes the model, data and parameters. Section 3 gives the simulation results with three architectures to transfer

energy from the VIPV to the main battery (through a 12 V battery, by means of a 48 V additional battery and directly in the high-voltage battery). Section 3.1 gives the results regarding PV energy transferred to the engine and the distance covered by the VIPV. Section 3.2 gives the results of the parametric study of the combination of PV peak power and thresholds for using PV. Section 3.3 gives the LCA results. Section 4 discusses the obtained results. Section 5 contains the conclusions of this study.

2. Materials and Methods

Most of the materials and methods are the same as the e-bus use case described in our paper [6] and published previously. The differences are the following:

- The curvature losses since passenger cars do not have a flat panel;
- The influence of the frequency of recharge with the grid;
- The sensitivity analysis regarding the electricity consumption of the electronics and the thresholds to use or not use the PV's energy;
- Three electrical architectures for charging the battery of the passenger car with the PV;
- The parameters of simulations, mainly PV surface, consumption in Wh per km, system efficiency, battery size, shading and use profile.

Figure 1 shows the inputs, outputs, parameters and the characteristics of the model simulating the PV energy transferred to the engine and the distance covered by the VIPV. The equations of the model are coded in a software developed by the authors in a Microsoft Excel environment. The Excel workbook contains several sheets: inputs (usage pattern and parameters); solar irradiance hourly distribution; monthly solar energy; equations; and 12 sheets for each month of the year. These last sheets consider the differences among the days for every month. To simulate the model, it is sufficient to modify only the sheet inputs. The values are, thus, automatically modified in the other sheets and the outputs are summarized in the output sheet.
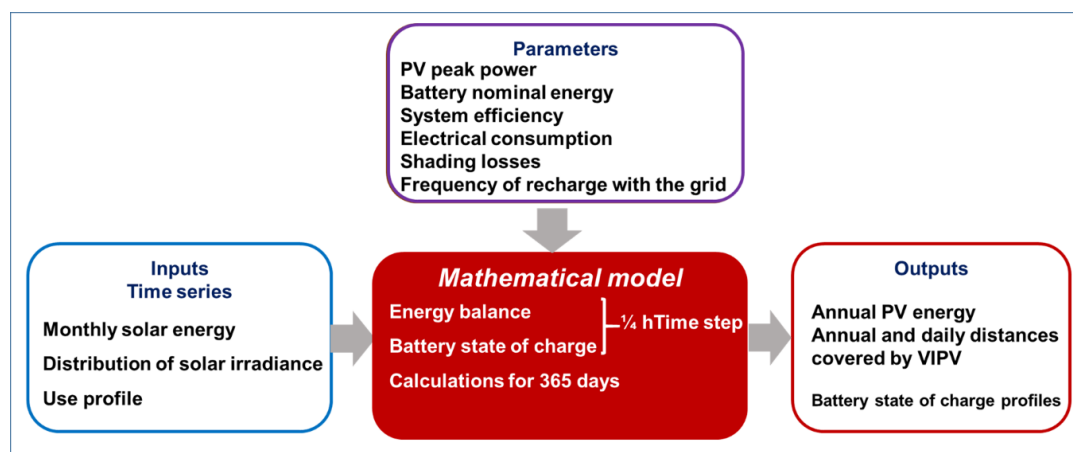

Figure 1. Energy and distance modeling.

2.1. Measurement and Calculation of Losses Due to the Curvature

The losses due to the curvature are measured as a function of the sun's elevation at the zenith for two solar panels with different curvatures in Chambéry, France. The experience consists of outdoor measurements of the maximum power point on one curved solar roof (radius of curvature approximately 3 m) and one standard flat reference module. The modules are placed facing south with 0° slope (horizontally). From August 2019 to February 2020, the measurements were recorded every 5 min during daytime. From this, an approximation of a linear regression of the producible loss versus the flat reference module as a function of the sun's elevation at the zenith was computed. This regression was extrapolated to compute the curvature losses for each location and according to the sun's elevation at the zenith through a typical year.

Equation (1) (Shivalingaswamy et al. [16]) calculates the sun's elevation at the zenith as a function of the co-latitude and the declination of the sun on the 15th of each month (*dayNum*).

$$\text{sun elevation at zenith} = 23.45 \times \sin\left(\frac{2 \times \pi \times (dayNum + 284)}{365}\right). \tag{1}$$

Therefore, the model calculates the losses due to the curvature on the 15th of every month for each city with the solar roofs considered.

As indicated previously [6] p. 3, the monthly photovoltaic producible values are obtained from the Photovoltaic Geographical Information System (PVGIS) [17] for a flat horizontal panel for 19 European cities. Considering the average and the highest annual PV productions among these cities, the chosen localities for VIPV studies are Paris and Malaga. Figure 2 shows the monthly PV produced energy in Malaga and Paris in kWh per kWp with and without curvature correction. The values for a flat panel are directly obtained from PVGIS. The subtraction of monthly curvature losses from the values for a flat panel yields the values for a curved panel. Total production, respectively, for a flat panel and a curved panel is 1635 kWh/kWp and 1535 kWh/kWp in Malaga and 1058 kWh/kWp and 965 kWh/kWp in Paris. The losses due to curvature are 8.8% in Paris and 6.1% in Malaga for a year.
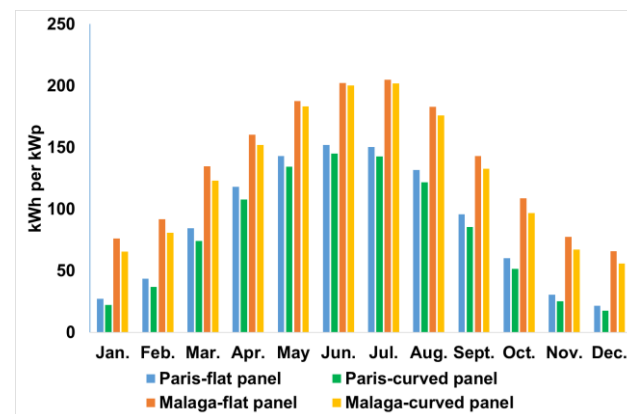

Figure 2. PV monthly production for 1 kWp for Paris and Malaga.

2.2. Electrical Architectures, System Efficiency and Thresholds

For a passenger car, three possible electrical architectures can transfer the PV energy into the vehicle's battery. These realistic architectures allow either charging the solar energy directly in the high-voltage (HV) battery or charging first a low-voltage (LV) battery and then intermittently transmitting the energy from the LV battery into the HV battery.

The PV system consumes additional energy, and the system's efficiency depends on the chosen architecture for charge. For a direct charge in the HV battery, this additional consumption is 12 W during driving and when plugging into the grid and 26 W during parking. For charging via a low-voltage auxiliary battery (12 V or 48 V), this consumption is constant at 12 W. In this case, there is a periodic wake-up (each 100 Wh) of the vehicle's calculators and the HV battery management system in order to transmit the electricity from the LV battery to the HV battery. The consumption is 8.5 Wh per wake-up.

The additional electricity consumption divided by the system's efficiency is equal to the thresholds applied to decide to trigger or not the PV use, which gives 13 W and 28 W for 12 W and 26 W extra consumption, respectively. The system transmits the PV energy to the battery only if the available power during the time step is higher than these thresholds. The model subtracted this additional electricity consumption from the PV's produced energy during all computing time steps. More details on the thresholds are in Section 3.2.1.

Table 1 gives the efficiency at each conversion and the total system efficiency for all architectures of a passenger car.

Table 1. System efficiency for a VIPV passenger car (2030 cases) for the three architectures considered.

Components	Via 12 V Battery	Via 48 V Battery	In Main Battery
DCDC (PV/LV battery)	99.1%	98.7%	NA
DCDC (LV/HV)	95.5%	97.5%	97.7%
MPPT	99%	99%	99%
LV battery	97%	97%	NA
DC/AC (battery/engine)	98.7%	98.7%	98.7%
HV battery	97%	97%	97%
System efficiency	87%	88.5%	92.6%

2.3. Use Profile and Parameters for Passenger Car

The consumption per km for a passenger car is estimated from the average of values referenced on the website [18]. It is 15.7 kWh/100 km or 157 Wh/km.

The model uses the use pattern (driving, parking, plugging) to calculate the consumption for all the days and all the computing time steps.

A passenger car is driven for a home/work trip: one hour in the morning (8 a.m.–9 a.m.) and one hour in the evening (5 p.m.–6 p.m.), 5 days per week and 48 weeks per year. Thus, a passenger car has long parking periods (8 h per day). This use pattern is defined with a car manufacturer, and it is a probable scenario for passenger cars. Discussion Section 4.4 quantifies the impact of the modification of this use pattern.

The considered battery size for a passenger car is 50 kWh.

The PV peak power used in the simulations at midlife considers a lifetime of the passenger car of 13 years and a PV degradation of −2% in the 1st year and then −0.7% per year. It is measured using INES facilities and is comparable to the values reported by Jordan et al. (2016) [19].

The two PV surfaces considered are the following:

- 1.44 m^2, value corresponding to covering 90% of the average surface of a passenger car's roof in France (1.58 m^2). This surface leads to 312 Wp at midlife when considering technological progress by 2030. The simulations in the Results section will be given with this value for the PV's surface;
- 2 m^2, value considered by Thiel et al. [7]. Section 4.3 will discuss the effect of such an increase in the PV's surface.

Simulations evaluate the daily PV produced by a panel with 49% and 30% shading factors. The value of 49% given by the European Commission [10] is mandatory for assessing the potential of VIPV but includes parking inside. The value of 30% is calculated using energy loss for a year in an urban driving environment when compared with stationary PV.

2.4. The Frequency of Recharge with the Grid

The simulations consider two occurrences of recharge with the grid: every night before a driving day and the maximal recharge frequency (*maxChargeFrequency*) depending on battery size (*storageEnergy*) and on the consumption of the vehicle (*dailyConsumption*). For this specific case, we obtained five days using Equation (2). Charging every five nights is enough for driving this passenger car for five days.

$$MaxChargeFrequency = \text{ROUNDDOWN}\left(\frac{80\% \times storageEnergy}{dailyConsumption}\right). \tag{2}$$

Equation (3) gives the state of charge profile of the battery using the method described in our previous work [6] (p. 6).

$$SOC_n = \max\left(\min\left(\frac{SOC_{n-1} \times energyStorage - cons + PVprod + gridCharge)}{energyStorage}, SOC_{max}\right), SOC_{min}\right). \quad (3)$$

SOC_n is the state of charge (SOC) at time step n; SOC_{n-1} is the SOC at time step $n-1$. SOC_{min} and SOC_{max} are the minimal and maximal SOC values, respectively. *energyStorage* is the battery's nominal energy or battery size in Wh. For the considered time step, *cons* is energy consumption (Wh), *PVprod* is PV energy net production (Wh) and *gridCharge* is the possible charge increment with the grid (Wh).

Here SOC_{max} is 100% and SOC_{min} is 0%.

The initial SOC is equal to SOC_{max}.

This calculation yields useful PV energy considering the influence of battery saturation.

3. Results

Here we present results for Paris and Malaga with three architectures of PV electricity transmission to the battery.

3.1. Results Regarding Energy and Distance Covered by VIPV

3.1.1. Simulation of the Quotidian Profiles

Figure 3 shows the electricity consumption and the PV production within a $\frac{1}{4}$ h time step and the state of charge (SOC) for a passenger car for two months. The consumption graphs are curtailed in order to zoom on production.

These graphs show the following:

- In January, the vehicle does not use the PV energy when it is lower than the thresholds associated with the additional consumption of electricity allowing the use of PV;
- In June, PV production is higher than these thresholds, but it is not used early in the morning because the battery is fully charged;
- The SOC profiles depend mostly on the use profile of the vehicle because consumption is much higher than production;
- There is a constant increase in the SOC during the night due to the recharge with the grid;
- For a passenger car, during the parking period, the increase in the battery's SOC is very low even in June.
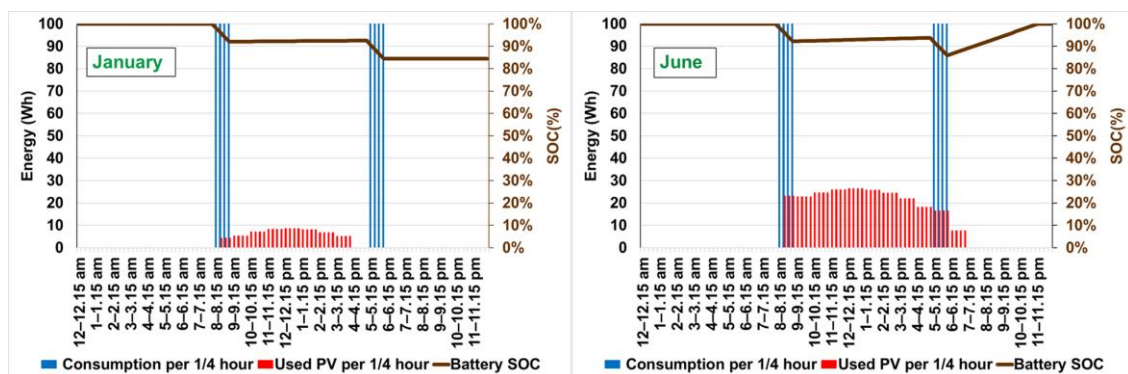

Figure 3. Examples of profiles, passenger car, direct charge in HV battery, Malaga, shading 30%.

3.1.2. Available Energy from the VIPV System

Figure 4 compares the performances of the three architectures to transfer the electricity from the solar roof to the battery of the passenger car with three values of shading share. The black column shows the annual photovoltaic energy correlated only to the solar irradiance

at the specific locality. There are three portions in the bar graph from the left side to the right side according to the three studied architectures.

The PV energies including the system's efficiency correspond to the yellow columns. They depend simply on the efficiency values given in Table 1. The other bars include the shading share influence and the effect of the thresholds (more detailed in Section 3.2.1). On these bars, two values are indicated according to including or not including the losses due to battery fullness. The battery may be full:

- In the morning, before driving due to plugging into the grid at night;
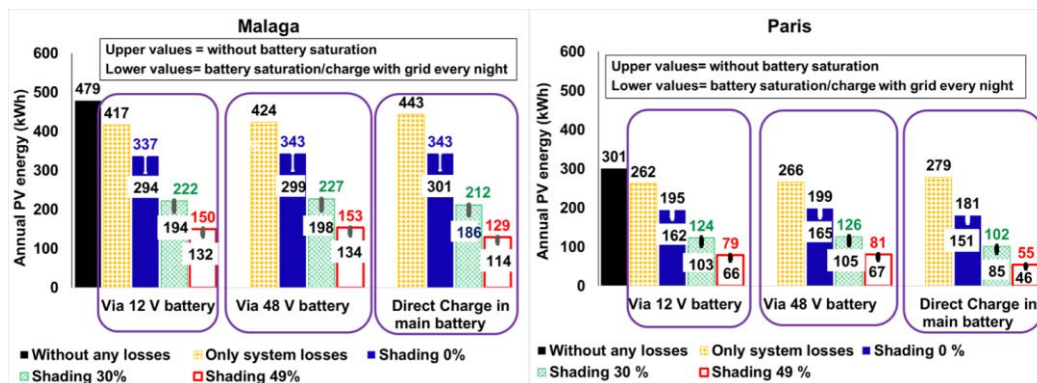- During rest days because there is no consumption due to driving.

Figure 4. Yearly PV energy in Malaga and Paris, passenger car, 0.312 kWp solar roof.

All the values used below are quantified on the graphs. The percentage calculated in Equation (4) compares two values *value*1 and *value*2.

$$percentage = \left| \frac{value2 - value1}{value1} \times 100 \right| \tag{4}$$

For example, to calculate the influence of battery saturation *value*1 without saturation (the upper values on the graph), *value*2 is with saturation (the lower values on the graph). Equation (4) yields *percentages* between 11% and 17%, depending on the use case. For example, in Paris with 49% shading and direct charge in the main battery, *value*1 = 55 and *value*2 = 46, so Equation (4) yields *percentage* = 16%.

The columns corresponding to shading share 0% (blue ones) in Figure 4 include the additional electricity consumption to transfer PV energy, which varies with the considered architecture and with the daylight duration. The impact of this consumption is relatively high when compared to the annual energy presented in the yellow columns. It is 98 kWh (54%) in Paris and 100 kWh (29%) in Malaga with direct charge of the HV battery from the VIPV system. It is 67 kWh (34%) in Paris and 80 kWh (24%) in Malaga for architectures with a charge via an LV battery. The percentage is relative to the PV's energy with 0% shading.

We can also see the following in Figure 4:

- The difference of energies between Malaga and Paris is about 70%. The locality has a major influence;
- The shading share is the second most important effect;
- There is extra-consumption to use the PV, so the thresholds have a third-order influence (24–54%) depending on the architecture and the location;
- The battery's fullness has a fourth-order influence (11–17%);
- The architecture with transfer through a 48 V battery is more effective than transfer through a 12 V battery, which is more effective than charging the HV battery directly (except with 0% shading in Malaga). However, its impact is of fifth-order (difference between architectures is only 7%). Changing the electrical architecture of recharge has

less influence than optimizing the thresholds. As indicated before, Section 3.2 will give a sensitivity study of the influence of the thresholds vs. peak power.

The blue bars are for shading equal to zero, which is not realistic in the case of a passenger car. Thus, the values up to are for the green bars, which include the system effectiveness, the additional consumption to transfer PV to the battery and a representative value of shading share. Readers can refer to the graphs to obtain the values with 0% shading. Thus, Figure 4 also shows the following:

- The best case: Malaga, 30% shading, charging through a 48 V battery and when battery is never full, the passenger car can gather up to 227 kWh;
- In Paris (~average Europe), passenger car can gather up to 126 kWh with 30% shading, when charging through the 48 V battery and when battery is never full and down to 46 kWh with 49% shading while charging the HV battery directly with the PV and a full battery.

Figure 5 presents the sensitivity of the model to the frequency of recharge for the case of direct transfer of the PV's energy to the HV battery.
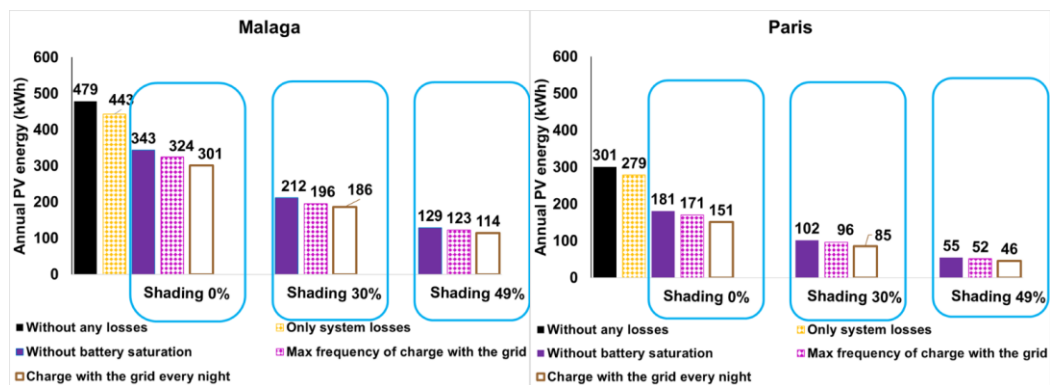

Figure 5. Yearly PV energy in Malaga and Paris, passenger car, 0.312 kWp solar roof, 50 kWh battery, direct transfer in the main battery, effect of frequency of recharge with the grid.

Figure 5 shows that the impact of recharge frequency is small, compared to other parameters. The difference between recharging with the grid every night and every five nights is 5% in Malaga and 12% in Paris with 30% shading share.

3.1.3. Yearly Distance Covered by VIPV

Figure 6 presents the simulation results of the model described in Figure 1 in terms of yearly distance covered by the VIPV system on a passenger car for the three-studied energy transfer architectures.
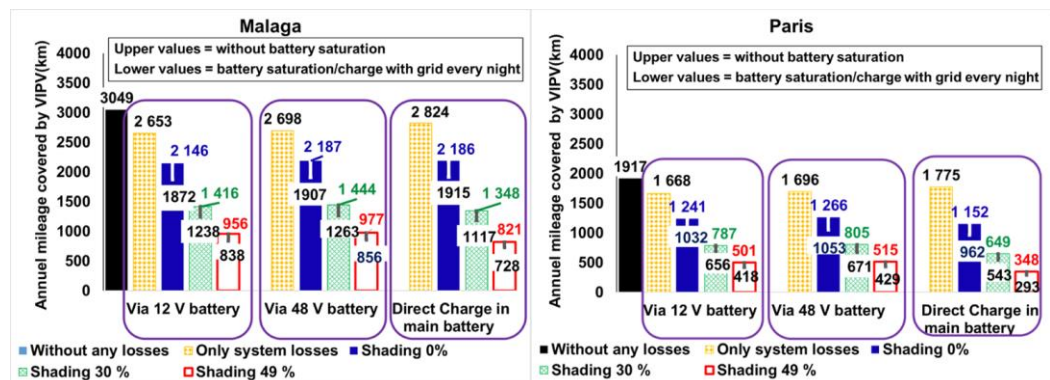

Figure 6. Yearly distance covered by VIPV in Malaga and Paris, passenger car, 0.312 kWp solar roof and 157 Wh/km electrical consumption.

Figure 6 shows that the VIPV can generate up to 1444 km per year at midlife in Malaga with 30% shading share and with transfer of energy through a 48 V battery. This distance represents 12% of the driven mileage (12,250 km). The range extension is down to 293 km per year in Paris with 49% shading share, direct charge of HV battery and with losses due to a full battery. It represents about 2% of the driven mileage. With the normalization of the results with the peak power of the solar roof, the annual mileage covered by the VIPV is up to 4628 km/kWp and down to 939 km/kWp.

Figure 7 presents the simulation results regarding the influence of the frequency of recharge for the case of directly charging an HV battery on the yearly distance covered by the VIPV. It shows that charging the battery with the maximal charging frequency (every 5 nights) obtains between 36 km and 151 km more than charging every night.
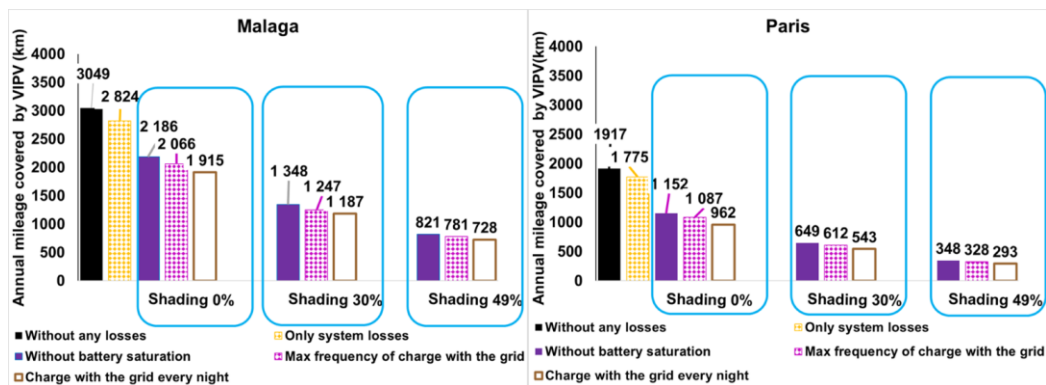

Figure 7. Yearly distance covered by VIPV in Malaga and Paris, passenger car, 0.312 kWp solar roof, 50 kWh battery, direct charge in HV battery, effect of plugging frequency.

3.1.4. Daily Distance Covered by the VIPV

Figure 8 presents the simulated average daily distance of VIPV on a passenger car for the three architectures of energy transfer considering battery saturation. When analyzing daily distance, values up to are without shading losses.
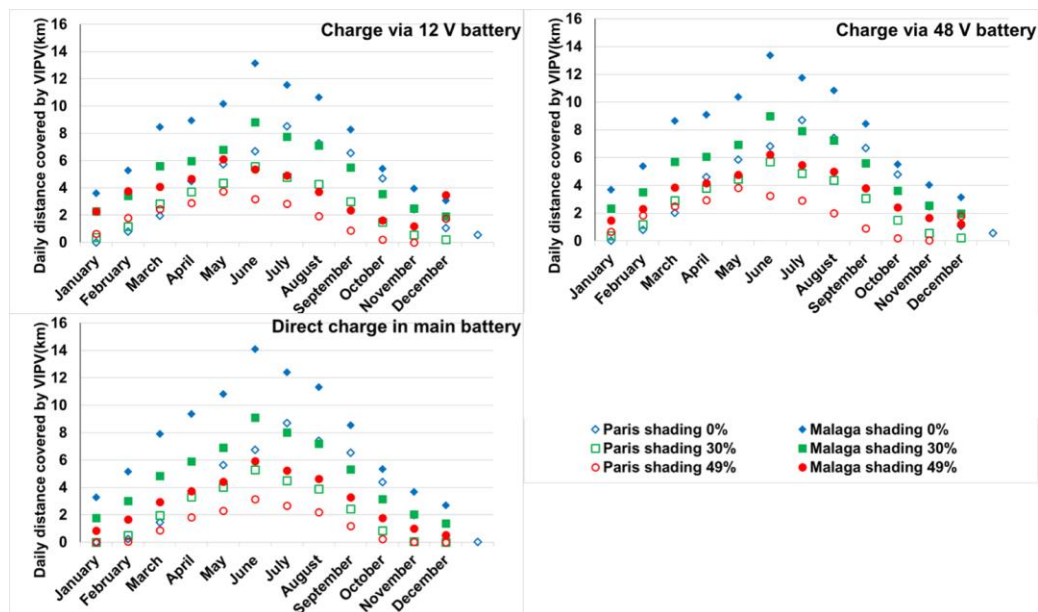

Figure 8. Average daily distance covered by VIPV, passenger car, 0.312 kWp solar roof and 157 Wh/km electrical consumption with battery saturation/charge with the grid every night.

Figure 8 indicates that for June, the sunniest month, the VIPV at midlife can cover an average distance up to 14 km/day (44 km/day/kWp) in Malaga, shading 0% and directly charging the main battery. The difference between architectures of energy transfer is less than 1 km. It shows, moreover, that in Paris (~average Europe), the VIPV can cover up to 8.7 km with 0% shading and 3.3 km with 49% shading.

3.2. Parametric Study of the Combination PV Peak Power/Thresholds Related to Electrical Architecture

3.2.1. Values of the Thresholds

In VIPV applications, PV energy has to be managed continuously: during parking and driving phases. Due to vehicle's electrical architecture, for safety or energy management reasons, dedicated electromechanical elements, such as an electronic control unit (ECU) or a battery management system (BMS), have to be switched-on to manage the energy flow from the PV panels to the battery. It results on power threshold values at a system level: below these values, the PV power from the panel is not available, due to a negative energy balance at the system level. In this context, the considered thresholds in energy predictions are the following:

- 13 W during the driving and parking phases. This is the most optimistic hypothesis (only one electromechanical relay on main battery);
- 13 W during driving and recharge with the grid phases and 28 W during the parking phase. This is the realistic hypothesis. During the parking phase, a partial wakeup of the vehicle is needed, which results in 28 W;
- 20 W during driving and charge with the grid phases and 40 W during the parking phase. These values were measured on a commercial electrical vehicle including VIPV.

The study of these three use cases allows a comparison of the energy performances and losses at a vehicular level.

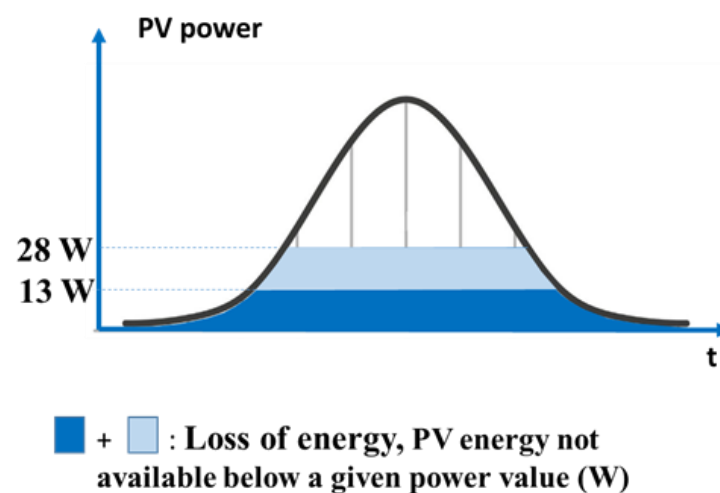Figure 9 presents an explanation of the threshold effect.

Figure 9. Graphical display of power threshold effect, schematic application onto a typical sunny day.

3.2.2. Analysis of the Combination of Peak Power/Thresholds

The simulated use cases are a combination of these thresholds with three values of peak power: 312 W, 433 W and 205 W. The other parameters are 30% shading and without battery saturation.

Figure 10 presents the simulation results for the cities of Malaga and Paris. For the calculation of the losses, the reference is the yellow bar including the system's efficiency and shading effects.
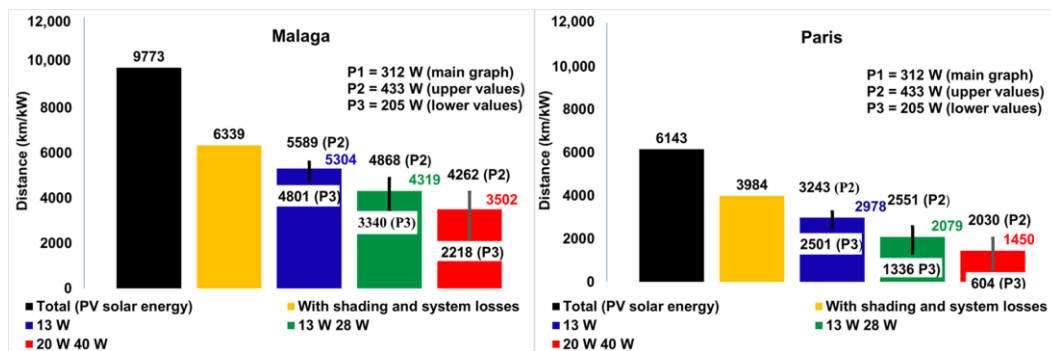
Figure 10. Yearly distance covered by VIPV in Malaga and Paris, passenger car, 30% shading, 157 Wh/km electrical consumption, with different peak power and threshold values.

Figure 10 shows the following:

- Lower peak power induces higher losses of PV energy and distance due to the thresholds. Therefore, even if the graphs present the distance per kW peak, the values are different in function of peak power;
- The losses due to the thresholds are very high. The minimum is 12% (Malaga, 433 W peak, threshold 13 W) and the maximum is 85% (Paris, 205 W peak, thresholds 20 W and 40 W);
- With the same shading level, the percentage of use of the PV depends on the location (1st order), the thresholds (2nd order) and the peak power (3rd order);
- The mileage covered by the VIPV per unit of peak power in Malaga is up to 5569 km/kW and down to 2218 km/kW depending on the peak power and the threshold values;
- The distance covered by VIPV per unit of peak power in Paris is between 604 and 3243 km/kW depending on the peak power and threshold values.

3.3. Life Cycle Assessment Results

The authors have described the methodology of life cycle assessment in a paper regarding the city bus use case [6] (pp. 7–10). In this paper, the same methodology of LCA is used for a passenger car. The main hypotheses are a low-carbon PV panel and not considering the end of life of the PV system. The main differences are the parameters regarding the PV surface, the additional weight, the lifetime of the vehicle and the additional battery in the case of charge via a 48 V battery.

3.3.1. Details of the Fabrication Phase

Table 2 presents the results of the fabrication phase for the three architectures.

Table 2. LCA results (fabrication phase) (kg CO_2-eq).

Component	Via 12 V Battery	Via 48 V Battery	In Main Battery
Total	76	139	76
PV module	62	62	62
Electronic/cable	13	27	13
Additional battery	NA	50	NA

3.3.2. Carbon Footprint Results

The estimation of the carbon footprint considers the fabrication and use phases of the vehicle. Regarding the use periods, the results are given in different localities according to the electricity mix and solar irradiance: both cities studied and average Europe, which has the same irradiance as Paris and average European electricity mix. The considered global warming scenario is set at +2.7 °C.
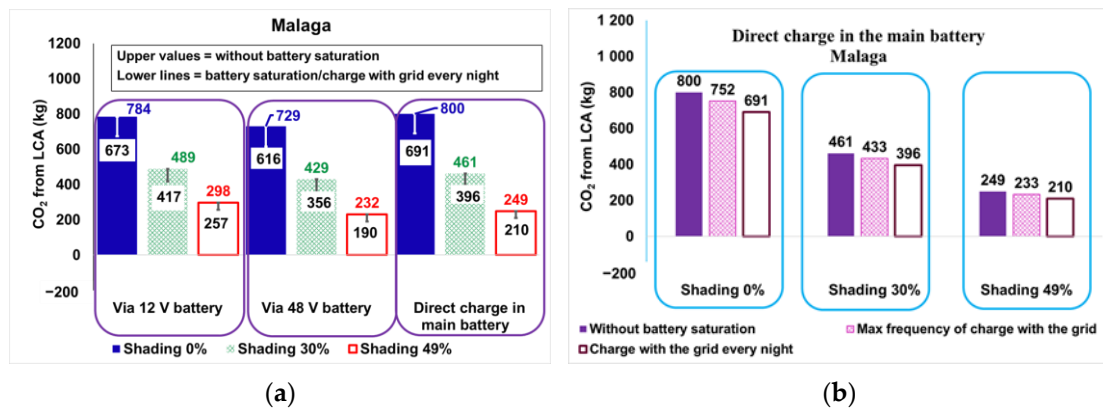
Figures 11–13 present life cycle assessment results.

Figure 11. Avoided emissions in Malaga, 0.312 Wp VIPV, global warming scenario +2.7 °C. (**a**) Graph with the three electrical architectures, (**b**) Graph for the impact of the frequency of recharge with the grid, architecture with direct transmission of PV electricity to the HV battery.
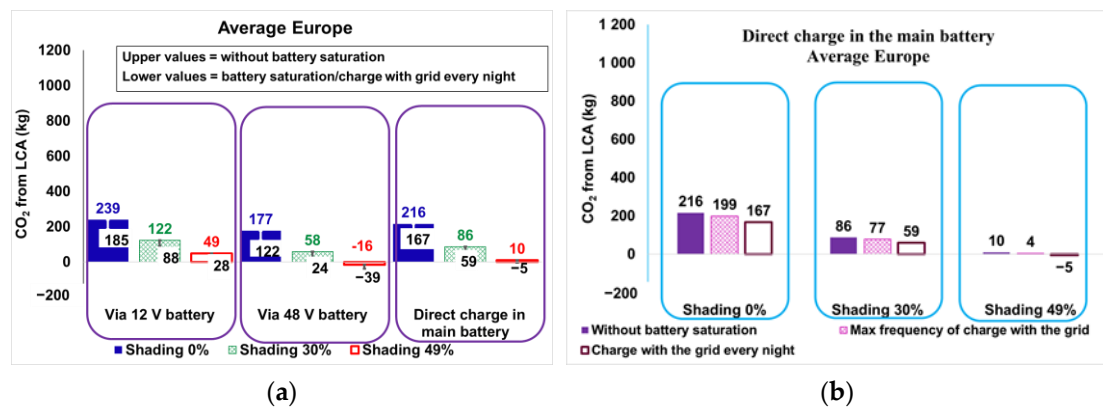

Figure 12. Avoided emissions in Average Europe, 0.312 Wp VIPV, global warming scenario +2.7 °C. (**a**) Graph with the three electrical architectures, (**b**) Graph for the impact of the frequency of recharge with the grid, architecture with direct transmission of PV electricity to the HV battery.
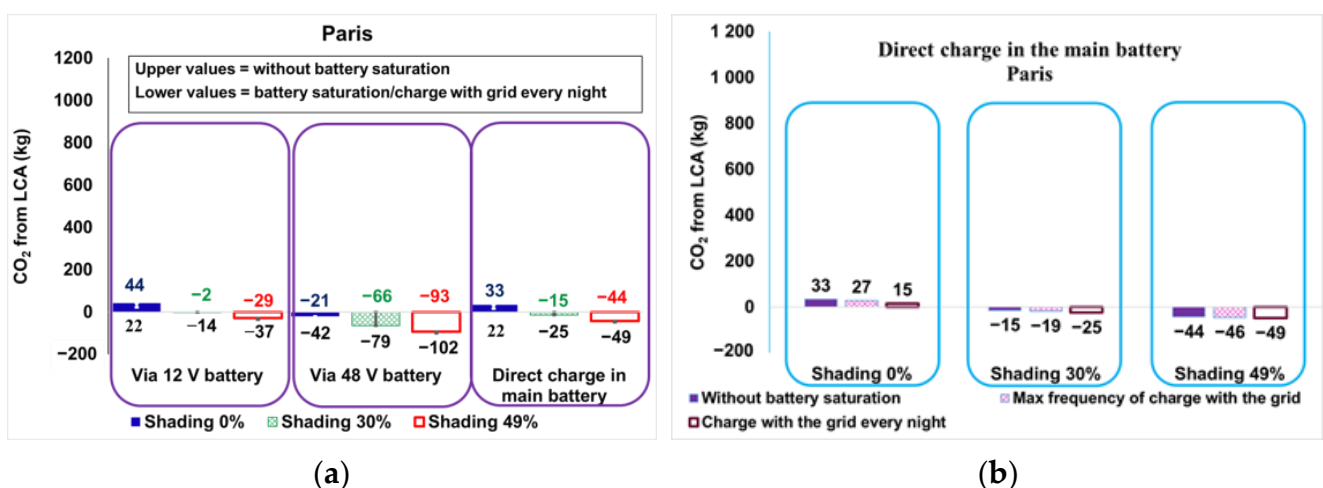

Figure 13. Avoided emissions in Paris, 0.312 Wp VIPV, global warming scenario +2.7 °C. (**a**) Graph with the three electrical architectures, (**b**) Graph for the impact of the frequency of recharge with the grid, architecture with direct transmission of PV electricity to the HV battery.

These figures show that in the case of the passenger car, VIPV may have a positive balance but not in all cities. The CO_2 balance depends mainly on the locality. With a very

low-carbon electricity mix in France, VIPV on a passenger car is not convincing. It has a negative CO_2 balance in Paris with 30% and 49% shading losses between -2 and -102 kg CO_2-eq. The best case in Europe avoids up to 489 kg CO_2-eq (Malaga, 30% shading and charge through 12 V battery). For average Europe, in terms of electricity mix and solar irradiance, VIPV may be not interesting because avoided emissions are 122 kg CO_2-eq in the best conditions (30% shading, charge through 12 V battery) and -39 kg CO_2-eq in the worst conditions.

4. Discussion

Several factors may improve vehicular performance, such as reducing the consumption of the vehicle per km, reducing the additional consumption for delivering PV electricity to the battery (i.e., the related thresholds) and improving the architecture for electricity transfer and PV peak power.

The car driver can optimize PV use by recharging less frequently with the grid and, of course, parking the vehicle preferably in sunny places.

The following subsections will discuss the impact of variable shading losses on the simulation results instead of constant shading losses, a bigger surface of the PV, lower system efficiency and some modifications on the use pattern. Finally, Section 4.5 presents a case study with an optimized PV surface and energy consumption per km.

4.1. Variable Shading vs. Constant Shading

This subsection first compares a constant shading value during a year with a variable value of shading between months with higher shading during winter compared to summer. These values of shading induce a loss of 30% of PV energy for one year in Paris. The values are estimated by geometric modelling with 10 m height buildings and with 11 m of route width in an urban environment considering the angle of incidence of the sunrays. Brito et al. [12] explained the variation in shading losses during a year and stated that the lower solar elevation in winter induces higher losses due to shading from buildings. Table 3 gives the shading values for a year in Paris. The values are between 21% and 69%. Araki et al. (2023) [20] investigated solar irradiance through a non-uniform shading object, coupled with a fisheye camera recording on a vehicle roof. The shading values recorded are from 11%, 27% and 46%, respectively, in an open zone, a residential zone and a building zone. A 30% shading scenario could be considered a generalized mean value.

Table 3. Variable shading losses between months in Paris.

January	February	March	April	May	June	July	August	September	October	November	December
69%	59%	29%	21%	23%	25%	24%	24%	23%	51%	69%	64%

Table 4 presents the simulation results with variable shading between months compared to constant shading in Paris. It shows an improvement between 0% and 9% of the energy used and of the distance covered by the VIPV. The improvement of life cycle assessment results is only between 1 and 2 kg CO_2-eq.

Another possibility to consider for the shading is different values between driving and parking. New simulated use cases are with shading losses equal to 26% during driving and 52% during parking, which are average yearly values for road and parking given by Brito et al. [12].

Table 5 presents the simulation results with shading differences between driving and parking as compared to a constant shading of 49% in Paris and Malaga for the three electrical architectures. The considered charge with the grid is every five nights.

Table 4. Simulation results with variable shading between months compared to constant shading of 30% in Paris.

Shading Losses		Variable between Months	30%	Evolution
PV useful energy per year (kWh)	Min	92	85	8%
	Max	129	126	2%
Mileage covered by VIPV per year (km)	Min	588	543	8%
	Max	822	805	2%
kg CO_2-eq	Min	−78	−79	1
	Max	0	−2	2
Mileage covered by VIPV (km/day)	Min	0	0	0%
	Max	6.2	5.7	9%

Table 5. Simulation results with different shading between driving and parking compared to constant shading of 49% in Paris and Malaga, energy in kWh.

Shading Losses		26% Driving/52% Parking	49%	Evolution
Charge via 12 V battery	Paris	73	74	−1%
	Malaga	139	142	−2%
Charge via 48 V battery	Paris	74	76	−3%
	Malaga	142	145	−2%
Direct charge in the main battery	Paris	51	52	−2%
	Malaga	119	123	−3%

Table 5 shows the small influence of considering different shading losses between the driving and parking phases. This is because the use profile of passenger cars includes parking most of the day.

4.2. Consequence of Lower System Efficiency

Table 6 presents the variation in PV energy used if the system's effectiveness is lower than the value used in the simulations above. The influence is not linear. When the system's efficiency is 13% lower, the PV energy used by the engine decreases between 20% and 25%. A 23% drop of such efficiency decreases the energy between 36% and 45%.

Table 6. Influence of lower system efficiency on useful PV energy, 30% shading; directly charging HV battery and battery never fully charged.

System Efficiency	Locality	PV Energy (kWh)	Evolution
93%	Paris	102	0%
	Malaga	212	0%
80%	Paris	77	−25%
	Malaga	170	−20%
70%	Paris	56	−45%
	Malaga	135	−36%

The difference between a passenger car and a city bus [6] is the relatively high influence of the thresholds to trigger or not the transfer of PV energy. It is due to a longer parking period and the energy produced is much lower for a passenger car than for a city bus.

4.3. Influence of PV Surface Increase

The solar roof surface considered for all the simulations above is 1.44 m². Car manufacturers may increase this surface in the future if they prefer to use the solar roofs only

on sedans with a bigger roof instead of all passenger cars. This subsection will discuss the effect a solar roof surface increase to 2 m^2. Thiel et al. consider this second value in the reference [7] as a solar roof surface for passenger cars. The consumption per km is not modified since the one considered is an average between smaller and larger cars. The surface of the roof, moreover, is not necessarily correlated with vehicle's weight and consumption. Only the surface is changed, and all the other parameters are fixed to distinguish the effect of the increase in the surface and, hence, of peak power.

Table 7 summarizes the results of the simulation with both solar roof surfaces in such conditions. It shows that such an increase in the surface induces 39% higher peak power. Regarding the yearly PV useful energy and the distance covered by the VIPV, it leads to a 31% increase in the max values and 47% of the min values. For the best month, the increase in the surface leads to a 33% increase in the max value and 39% increase in the min value.

Table 7. Comparison of the values for two surfaces of a solar roof for a passenger car.

PV Surface		1.44 m^2	2 m^2	Evolution
PV peak power (kW)		0.312	0.433	39%
PV useful energy per year (kWh)	Min	46	87	47%
	Max	227	326	30%
Distance covered by VIPV per year (km)	Min	293	554	47%
	Max	1444	2078	31%
Distance covered by VIPV Best month (km/day)	Min	3.3	5.4	39%
	Max	14	20.9	33%

With a 2 m^2 solar roof, for the best case in Europe (Malaga, 30% shading, architecture of energy transfer through a 48 V battery and without losses due to a full battery), the driver obtains 2078 km per year at midlife of the vehicle, which represents 17% of the driven distance during a year. The auto-generated distance for the best month is ~21 km in this case; in addition, the driver has almost 42% of the daily distance (~50 km).

4.4. Influence of Modification of the Use Profile

The model is simulated with two modifications of the use profile. The simulated use case is Paris (~average Europe), 30% shading losses, direct charge in the main battery, charge with the grid every five days. The first modification is the addition of a roundtrip Saturday afternoon: driving 5 p.m.–6 p.m. and 7 p.m.–8 p.m. In this case, the yearly distance covered by the VIPV is 614 km instead of 612 km with only a home/work roundtrip. The influence is about 0.3%, which is not significant. The second modification presented in Figure 14 is the addition of a long distance trip (600 km) during Saturday of holiday periods and two rapid charges during these days. The yearly distance covered by the VIPV is 608 km, which is 1.1% lower than the considered use profile in this paper.
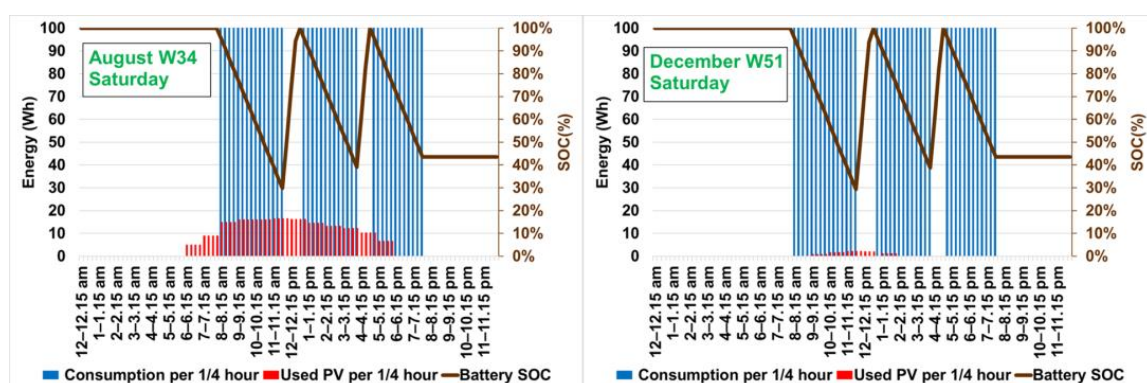

Figure 14. Profiles for long distance trip, direct charge in HV battery, Paris, shading 30%.

4.5. Simulation of the "Lightyear" Use Case

Many factors can influence the performance and gains obtained with a VIPV system on a passenger car. The existing vehicles with a high level of consumption per km and a high influence of the thresholds due to extra-consumption to charge PV energy in the battery have low performances. It is interesting here to simulate a use case with a reduction in the consumption per km, with a large surface of PV and with a small consumption of the electrical architecture as compared to PV installed power. For this, the considered consumption is 109 Wh/km, the value given for a Lightyear 0 vehicle [21]. The battery size of this vehicle is 60 kWh, and the solar roof peak power is 1.05 kW.

First, simulations allow the comparison of the annual energies of the VIPV system normalized for 1 kW at midlife between the vehicle with 0.312 kWp and Lightyear 0. The previous vehicle is a solarized electric vehicle, which has the characteristics of average existing electric vehicles in terms of consumption (157 Wh/km), roof surface (1.44 m^2) and battery size (50 kWh). Solarizing here means adding a VIPV system to an existing electric vehicle model. The Lightyear 0 is a vehicle integrating solar since its conception. Equation (2) in Section 2.4 yields eight as a maximal frequency of recharge with the grid of this vehicle. Thus, the model considers a charge with the grid only every eight nights. For the case of an average solarized electric vehicle, the considered charge with the grid is every five nights. Table 8 shows the results of the comparison of these configurations between a Lightyear vehicle and a solarized vehicle.

Table 8. Percentage of increase in energy per kWp for a solar vehicle (Lightyear 0 main characteristics) compared to a solarized electric vehicle's performance.

	Only System Losses	Shading 0%	Shading 30%	Shading 49%
Charge via 12 V battery	0%	10%	21%	35%
Charge via 48 V battery	0%	9%	20%	33%
Charge in the main battery	0%	27%	55%	97%

Table 8 shows that the useful energy's variation is not linear. It is due to the thresholds related to extra consumption of the vehicle to use the PV's energy as explained in Section 3.2. The higher peak power can even double the useful energy per kWp in the case of a high shading level and directly charging the HV battery.

Figure 15 shows the yearly distance covered by VIPV in Paris for a solar vehicle with the main characteristics of Lightyear 0 in terms of solar roof peak power, energy consumption per km, battery nominal energy and with grid recharge every eight nights.
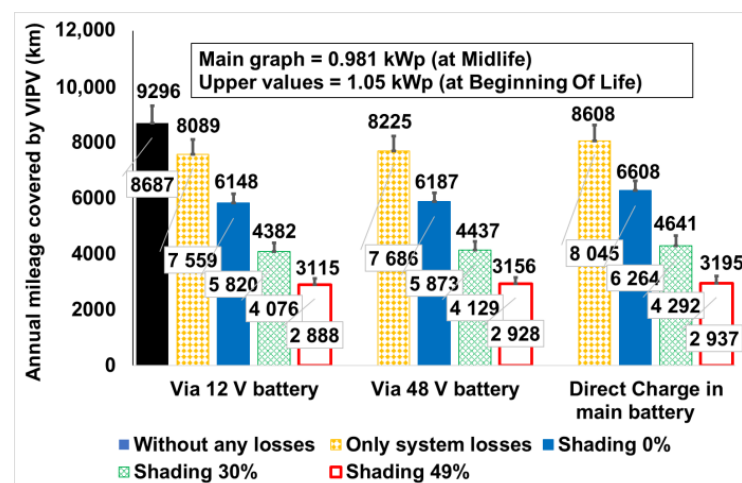

Figure 15. Yearly distance covered by VIPV in Paris with Lightyear 0 main characteristics 0.981 kWp (Midlife)/1.05 kWp (BOL) solar roof, 109 Wh/km consumption and 60 kWh battery.

This figure shows that the values are much higher than in the case of a solarized electric vehicle. In the worst case, in terms of shading level and in average Europe in terms of irradiance, the solar electric vehicle with the characteristics of Lightyear 0 can cover 2888 km. This is due to the cumulative effect of high peak power, which is discussed above, and to low consumption per km. Unfortunately, the company which manufactured the Lightyear 0 vehicle declared bankruptcy in January 2023 [22]. One of the causes may be the high price (€250,000) and small production volume of this vehicle. Solarizing existing electrical vehicles has the advantage of affordable cost, enabling large selling volumes and the inconvenience of low performances. Therefore, multiplying the carbon footprint by a large number of vehicles gives a positive balance under favorable conditions.

5. Conclusions

This study analyzed the performances of VIPV on a passenger car. The three systems considered to transfer the energy from VIPV to the battery are a system charging directly the HV battery and systems charging a 12 V or a 48 V battery before intermittent transmission of the electricity in the HV battery.

Simulations indicate the order of influence of the parameters on the outputs of the numerical model presented in this paper: geographic position (1st order), shading (2nd order), thresholds related to extra-consumption of the VIPV system (3rd order), frequency of recharge with the grid (4th order) and the electric architecture (5th order). A system charging through a 48 V battery enables higher mileage but has a lower performance in terms of the LCA due to the additional battery. Direct charge of the HV battery may be a compromise between performances in terms of mileage, complexity and carbon balance.

In Europe, in sunny cities like Malaga, VIPV on a passenger car can gather up to 227 kWh per year at midlife with 312 Wp and 30% shading with an intermediate 48 V battery. It covers up to 1444 km in annual distance. This represents 12% of the vehicle's needs. For the best month, it can cover up to 14 km per day. For cities similar to average Europe, a passenger car can gather only 46 kWh per year, which covers only 293 km of yearly distance, with 312 Wp and 49% shading. For the most realistic scenario in 2030, with direct charge in an HV battery, 312 Wp, 30% shading and Paris irradiance (mean value Europe), the result is 101 kWh or 648 km per year.

Specific VIPV development for energy optimization, such as a Lightyear 0 vehicle, considering 981 Wp at midlife (1.05 Wp installed) with 30% shading, can generate 4292 km per year. This clearly highlights that VIPV have to be considered at the beginning of the vehicle's conception to fully optimize VIPV benefits.

Based on yearly PV energy and the mileage covered by VIPV, life cycle assessment was carried out with a low-carbon PV module and system hypotheses. The electricity mix and the solar irradiance have a high impact on the final CO_2-eq. balance. The best European scenario is Malaga, coupled with a relatively highly carbonized electricity mix (up to 489 kg CO_2-eq avoided). The worst scenario is Paris, with a low carbon electricity mix (France). The CO_2-eq balance remains negative at 13 years of the vehicle's lifetime. The realistic scenario considered includes a European electricity mix, coupled with average European solar irradiance. In these conditions, the final CO_2-eq balance is 77 kg CO_2-eq, close to neutral. Beyond auto-generated distance and LCA topics, VIPV on passenger cars could be more efficient in specific applications, such as a fully dedicated VIPV vehicle, a light vehicle or collective mobility solutions, or, for specific environments such as non-interconnected zones and for resilience in the case of natural catastrophes as indicated by Araki et al. (2023) [23].

Abbreviations

The following abbreviations are used in this manuscript:

BMS	Battery Management System
BOL	Beginning of Life
CO_2-eq	Carbon Dioxide Equivalent
ECU	Energy Control Unit
EVs	Electrical Vehicles
HV	High Voltage
JRC	European Commission's Joint Research Centre
LCA	Life Cycle Assessment
LV	Low Voltage
PV	Photovoltaics
SOC	State of Charge
VIPV	Vehicle Integrated Photovoltaics

References

1. European Commission Press Release. Available online: https://ec.europa.eu/commission/presscorner/detail/en/ip_22_6462 (accessed on 2 November 2022).
2. Mawonou, K.S.R.; Eddahech, A.; Dumur, D.; Beauvois, D.; Godoy, E. State-of-Health Estimators Coupled to a Random Forest Approach for Lithium-Ion Battery Aging Factor Ranking. *J. Power Sources* **2021**, *484*, 229154. [CrossRef]
3. Shen, X.; Zhao, H.; Xiang, Y.; Lan, P.; Liu, J. Short-Term Electric Vehicles Charging Load Forecasting Based on Deep Learning in Low-Quality Data Environments. *Electr. Power Syst. Res.* **2022**, *212*, 108247. [CrossRef]
4. Jirdehi, M.A.; Tabar, V.S. Multi-Objective Long-Term Expansion Planning of Electric Vehicle Infrastructures Integrated with Wind and Solar Units under the Uncertain Environment Considering Demand Side Management: A Real Test Case. *Sustain. Cities Soc.* **2023**, *96*, 104632. [CrossRef]
5. Commault, B.; Duigou, T.; Maneval, V.; Gaume, J.; Chabuel, F.; Voroshazi, E. Overview and Perspectives for Vehicle-Integrated Photovoltaics. *Appl. Sci.* **2021**, *11*, 11598. [CrossRef]
6. Karoui, F.; Claudon, F.; Chambion, B.; Catellani, S.; Commault, B. Estimation of Integrated Photovoltaics Potential for Solar City Bus in Different Climate Conditions in Europe. *J. Phys. Conf. Ser.* **2023**, *2454*, 012007. [CrossRef]
7. Thiel, C.; Gracia Amillo, A.; Tansini, A.; Tsakalidis, A.; Fontaras, G.; Dunlop, E.; Taylor, N.; Jäger-Waldau, A.; Araki, K.; Nishioka, K.; et al. Impact of Climatic Conditions on Prospects for Integrated Photovoltaics in Electric Vehicles. *Renew. Sustain. Energy Rev.* **2022**, *158*, 112109. [CrossRef]
8. Sagaria, S.; Duarte, G.; Neves, D.; Baptista, P. Photovoltaic Integrated Electric Vehicles: Assessment of Synergies between Solar Energy, Vehicle Types and Usage Patterns. *J. Clean. Prod.* **2022**, *348*, 131402. [CrossRef]
9. Lodi, C.; Seitsonen, A.; Paffumi, E.; De Gennaro, M.; Huld, T.; Malfettani, S. Reducing CO_2 Emissions of Conventional Fuel Cars by Vehicle Photovoltaic Roofs. *Transp. Res. Part D Transp. Environ.* **2018**, *59*, 313–324. [CrossRef]
10. Commission Implementing Decision of 18 November 2014. Available online: https://eur-lex.europa.eu/legal-content/EN/TXT/PDF/?uri=CELEX:32014D0806&rid=1 (accessed on 4 April 2023).

11. Arun, P.; Mohanrajan, S. Effect of Partial Shading on Vehicle Integrated PV System. In Proceedings of the 3rd International Conference on Electronics, Communication and Aerospace Technology (ICECA), Coimbatore, India, 12–14 June 2019; pp. 1262–1267. [CrossRef]

12. Brito, C.-M.; Santos, T.; Moura, F.; Pera, D.; Rocha, J. Urban Solar Potential for Vehicle Integrated Photovoltaics. *Transp. Res. Part D Transp. Environ.* **2021**, *94*, 102810. [CrossRef]

13. Ota, Y.; Araki, K.; Nagaoka, A.; Nishioka, K. Curve Correction of Vehicle-Integrated Photovoltaics Using Statistics on Commercial Car Bodies. *Prog. Photovolt. Res. Appl.* **2022**, *30*, 152–163. [CrossRef]

14. Ota, Y.; Araki, K.; Nagaoka, A.; Nishioka, K. Facilitating Vehicle-Integrated Photovoltaics by Considering the Radius of Curvature of the Roof Surface for Solar Cell Coverage. *Clean. Eng. Technol.* **2022**, *7*, 100446. [CrossRef]

15. Birnie, D.P. Analysis of Energy Capture by Vehicle Solar Roofs in Conjunction with Workplace Plug-in Charging. *Sol. Energy* **2016**, *125*, 219–226. [CrossRef]

16. Shivalingaswamy, T.; Kagali, B.A. Determination of the Declination of the Sun on a Given Day. *Eur. J. Phys. Educ.* **2012**, *3*, 17–22.

17. JRC Photovoltaic Geographical Information System (PVGIS)—European Commission. Available online: https://re.jrc.ec.europa.eu/pvg_tools/en/#api_5.1 (accessed on 8 October 2021).

18. Hello Watt. Available online: https://www.hellowatt.fr/suivi-consommation-energie/consommation-electrique/consommation-recharge-voiture-electrique (accessed on 15 November 2021).

19. Jordan, D.C.; Kurtz, S.R.; VanSant, K.; Newmiller, J. Compendium of Photovoltaic Degradation Rates. *Prog. Photovolt. Res. Appl.* **2016**, *24*, 978–989. [CrossRef]

20. Araki, K.; Ota, Y.; Nagaoka, A.; Nishioka, K. 3D Solar Irradiance Model for Non-Uniform Shading Environments Using Shading (Aperture) Matrix Enhanced by Local Coordinate System. *Energies* **2023**, *16*, 4414. [CrossRef]

21. EV-Data Base. Available online: https://ev-database.org/car/1166/Lightyear-0 (accessed on 15 May 2023).

22. Carexpert. Available online: https://www.carexpert.com.au/car-news/lightyear-solar-powered-ev-enters-production (accessed on 15 May 2023).

23. Araki, K.; Ota, Y.; Maeda, A.; Kumano, M.; Nishioka, K. Solar Electric Vehicles as Energy Sources in Disaster Zones: Physical and Social Factors. *Energies* **2023**, *16*, 3580. [CrossRef]